Biochemical and Biophysical Research Communications 464 (2015) 548–553

Contents lists available at ScienceDirect

Biochemical and Biophysical Research Communications

journal homepage: www.elsevier.com/locate/ybbrc

Novel insights into the apoptosis mechanism of DNA topoisomerase I inhibitor isoliquiritigenin on HCC tumor cell

Ze-xin Li, Jian Li, Yan Li, Kun You, Hongwei Xu, Jianguo Wang*

Department of General Surgery, The First Affiliated Hospital of Xinxiang Medical University, 453100, China

ARTICLE INFO

Article history:
Received 25 June 2015
Accepted 1 July 2015
Available online 6 July 2015

Keywords:
Isoliquiritigenin
DNA topoisomerase I
Inhibition effect
Fluorescence quenching
Melting measurements
Molecular simulation
Apoptosis cells

ABSTRACT

The inhibitory effect of DNA topoisomerase (Top I) by isoliquiritigenin(ISO) were investigated and their interaction mechanism was evaluated using methods including UV–vis absorption, fluorescence, coupled with molecular simulation, and using the MTT method of inhibition rate of HCC tumor cell SNU475 proliferation assay, finally, the interaction of ISO with calf thymus DNA was investigated by melting measurements and molecular docking studies. It was found that isoliquiritigenin reversibly inhibited DNA Top I in a competitive manner with the concentrations of ISO resulting in 50% activity lost (IC_{50}) were estimated to be 0.178 ± 0.12 mM. Isoliquiritigenin exhibited a strong ability to quench the intrinsic fluorescence of Top I through a static quenching procedure. The positive values of enthalpy change and entropy change suggested that the binding of isoliquiritigenin to Top I was driven mainly by hydrophobic interactions. The molecular docking results revealed isoliquiritigenin actually interacted with the primary amino acid residues on the active site of Top I, and the detection results of fluorescence staining and the inhibitory effect on the growth of HCC SUN475 showed that isoliquiritigenin induced the apoptosis cells increased gradually. The interaction of ISO with DNA can cause the denaturation temperature to be increased, which indicated that the stabilization of the DNA helix was increased in the presence of ISO, which indicated that the results provide strong evidence for intercalative binding of ISO with DNA.

1. Introduction

The topoisomerase I (Top I) family of eukaryotic enzymes is required to relax DNA supercoiling generated by replication, transcription, and chromatin remodeling [1–4]. Human Top I acts through a nucleophilic tyrosine residue (Tyr723), which nicks the phosphodiester backbone of double-stranded, supercoiled DNA and forms a transient cleavage complex in which the 3′end of the broken DNA strand is covalently linked to the enzyme [5–8]. Camptothecin is a natural product for which Top I is its only cellular target [9]. Two camptothecin derivatives, irinotecan and topotecan, are the only current Top I inhibitors approved by the U.S. Food and Drug Administration for the treatment of cancer [10,11]. However, these camptothecin derivatives have several major drawbacks. First, camptothecins are compromised by the reversibility of the Top1-DNA cleavage complex, which necessitates long infusion times for maximum activity [12–14]. Second, the lactone ring is inherently unstable and hydrolyzes to form an inactive hydroxy acid [15,16]. In addition, the anticancer activities of the camptothecins are compromised by R364H [17] and N722S [18] mutations as well as by induction of the ABCG2 [19–21] and MXR [21] ATP-binding cassette drug efflux transporters. Myelosuppression is dose-limiting with topotecan [22], whereas the major dose-limiting toxicities of irinotecan are neutropenia and diarrhea [23]. These limitations have stimulated the search for non-camptothecin Top I inhibitors as anticancer agents.

Isoliquiritigenin(Fig. 1A) was found to be a Top I inhibitor with anticancer activity in the National Cancer Institutes 60 (NCI60)-cell screen indicated a high degree of correlation with camptothecin. Subsequent studies confirmed that the mechanism of action of the isoliquiritigenin is identical to that of the camptothecins. Specifically, they stabilize the ternary cleavage complex by intercalation between the DNA base pairs at the cleavage site after single-strand cleavage by Top I, thus preventing religation of the broken phosphodiester backbone, which are therefore classified as Top I poisons as opposed to Top I suppressors, which inhibit the DNA cleavage reaction.

* Corresponding author.
E-mail address: wangjianguoxx@163.com (J. Wang).

http://dx.doi.org/10.1016/j.bbrc.2015.07.003
0006-291X/

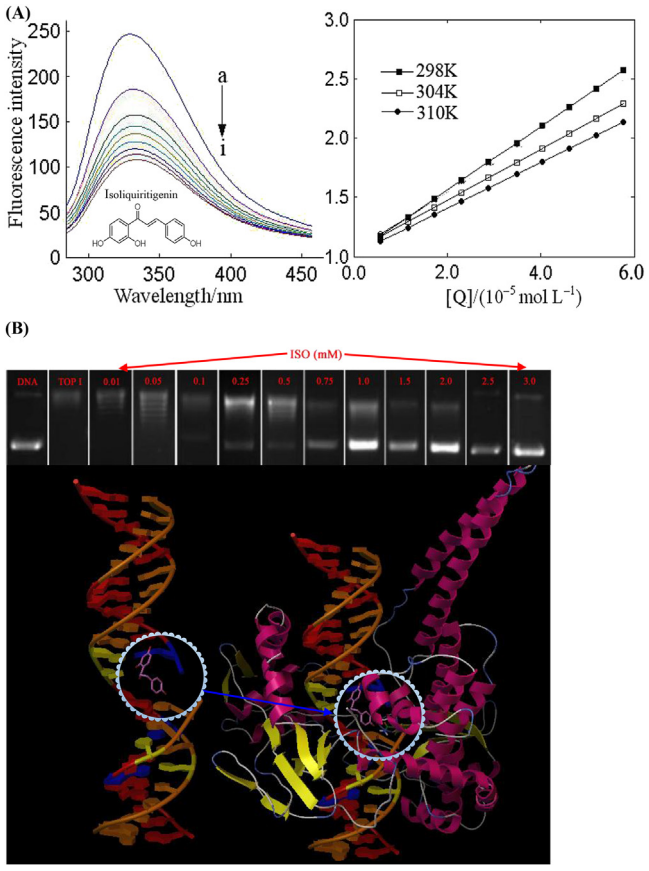

Fig. 1. (A) Fluorescence spectra of TOP I in the presence of ISO at different concentrations (pH 7.0, $T = 298$ K, $\lambda_{ex} = 280$ nm, $\lambda_{em} = 341$ nm). c(TOP I) $= 2.0 \times 10^{-6}$ M, and c(ISO) = 0, 0.3, 0.6, 0.9, 1.2, 1.5, 1.8, 2.1, and 2.4 mM for curves a→i, respectively; The Stern–Volmer plots for the fluorescence quenching at different temperatures. (B) Dose dependent inhibitory profile of ISO on TOP I; DNA-blank (supercoiled DNA); TOP I-(supercoiled DNA + TOP I + DMSO); ISO-(supercoiled DNA + TOP I + ISO at varied concentrations in DMSO), and the predicted binding mode of ISO docked with TOP I.

2. Materials and methods

2.1. Fluorescence spectra measurements

Fluorescence (F-7000, Hitachi) measurements were measured at different temperatures (298, 304, and 310 K) in range of 300–500 nm with an excitation wavelength at 280 nm, and the excitation and emission bandwidths were both set at 2.5 nm. Appropriate blanks corresponding to the buffer are subtracted to correct background fluorescence.

In the present work, the following relationship was used to correct the inner-filter effect [24]:

$$F_c = F_m e^{(A_1+A_2)/2} \quad (1)$$

where F_c and F_m are the corrected and measured fluorescence, respectively. A_1 and A_2 are the absorbance of ISO at excitation and emission wavelengths, respectively.

The fluorescence quenching data were analyzed by the Stern–Volmer equation [25]:

$$\frac{F_0}{F} = 1 + K_{SV}[Q] = 1 + K_q t_0[Q] \quad (2)$$

where F_0 and F are the fluorescence intensities (344 nm) of Top I in the absence and presence of quencher, respectively. K_{SV} is the Stern–Volmer quenching constant ($K_{SV} = K_q \tau_0$), K_q is the quenching rate constant of biomolecule, [Q] is the concentration of ISO. τ_0 is the average lifetime of the fluorophore without quencher, and the value of τ_0 of the biopolymer is 10^{-8} s [26].

The binding constant (K) and the number of bound ISO to TOP I (n) were determined by the following equation [27]:

$$\log \frac{F_0 - F}{F} = \log K + n \log[Q] \quad (3)$$

If the temperature does not vary significantly, the enthalpy change (ΔH°) can be regarded as a constant, then its value and entropy change (ΔS°) value can be evaluated from the van't Hoff equation as follows:

$$\log K_a = -\frac{\Delta H^\circ}{2.303RT} + \frac{\Delta S^\circ}{2.303R} \quad (4)$$

where R is the gas constant, and the temperatures used were 298, 304, and 310 K. The value of free energy change (ΔG°) can be obtained from the following equation:

$$\Delta G^\circ = \Delta H^\circ - T\Delta S^\circ \quad (5)$$

2.2. In-vitro enzyme inhibition study

In nature, usually plasmids exist as negatively supercoiled forms. Supercoiled pUC 19 was used as the substrate for relaxation assays. IU of enzyme was defined as the least quantity of the TOP I enzyme required for complete relaxation of 0.5 μg of negatively supercoiled plasmid pUC 19 DNA in 30 min at 37 °C [28]. The DNA relaxation assay was performed in a standard reaction volume of 30 μL assay buffer with 10 mM Tris–HCl (pH 7.0), 50 mM NaCl, 6 mM $MgCl_2$, 0.1 mg/mL gelatin and 0.5 μg of supercoiled pUC 19 plasmid DNA (HiPurA plasmid DNA maxiprep purification spin kit, HiMedia). Reactions were initiated by adding 800 ng TOP I protein. Later, after incubation at 37 °C for 30 min, the reactions were quenched by adding 5 μL of Stop buffer (50 mM EDTA (pH 7.0); 50% glycerol and 0.5% (v/v) bromophenol blue). Subsequently, the DNA was electrophoresed in a 1% (w/v) agarose gel with TAE buffer. The gels were stained after the electrophoresis to prevent any differences in mobility of DNA due to chelation; gel was stained with ethidiumbromide and photographed over UV light using GelDoc imager (Bio-Rad). The supercoiled plasmid was considered as blank; the supercoiled DNA with the TOP I enzyme was used as control with 100% relaxation. Different concentrations of the ISO tested were assayed to know the percentage inhibitions on the enzyme.

2.3. In-vitro cytotoxicity screening

ISO was further screened for cytotoxic activity using Human HCC tumor cell line (SUN 475) at 25 μM. The cells were grown in RPMI medium with 10% FBS. The activity was carried out using MTT assay. The enzymes in the viable cell have the capability of reducing the tetrazolium dye MTT to its reduced form formazon, which has purple color. The cells were grown in RPMI-1640 medium supplemented with 10% FBS (Fetal bovine serum), 100 IU/mL penicillin, 100 mg/mL streptomycin and 2 mM glutamine. Cell line was maintained at 37 °C in a humidified 5% CO_2 incubator. Cells were scrapped and seeded into wells approx 5000 cells per well in poly-L-lysine coated plates. The plates were incubated at 37 °C in humidified CO_2 incubator and then treated with the synthesized compounds at 25 μM concentration and incubated for 48 h. 10 μL of 0.5 mg/mL concentration of MTT was added and incubated for 3 h

at 37 °C and the final product formazon crystals were dissolved in 100 μL of DMSO and the viability was measured at 595 nm.

2.4. DNA melting studies

The melting temperatures of DNA and ISO–DNA complex were measured by monitoring the absorption intensities at 260 nm of samples at various temperatures. The absorbance intensities were then plotted as a function of temperature ranging from 20 to 100 °C. The melting temperatures (T_m) of DNA and ISO–DNA complex were determined as the transition midpoint.

2.5. Molecular docking studies

The 3D structure of ISO was generated in Sybyl × 1.1 (Tripos Inc., St. Louis), its energy-minimized conformation was obtained with the help of the MMFF94 force field using MMFF94 charges, and the TOP I(PDB: 1T8I), DNA(PDB: 453D) [29] model were used as the receptor model in the virtual screening with docking simulations. All the water molecules were removed, the polar hydrogen atoms and kollman charges were added to the TOP, DNA model, the grid maps for energy scoring were calculated using AutoGrid. Docking calculations were performed using the default parameters (runs 100) and the rotatable bonds in the ligand were assigned with AutoDock Tools, and the ligand docking was performed with the AutoDock 4.2 [30] Lamarckian Genetic Algorithm (LGA), and output from AutoDock was rendered with PyMol.

2.6. Statistical analysis

The experimental results was expressed as mean value ± standard deviation ($n = 3$), and data were analyzed using the SAS statistical package (version 8.1, SAS Institute, Cary, NC, USA).

3. Results and discussion

3.1. Fluorescence quenching studies of TOP I by ISO

Fig. 1A shows that the fluorescence intensity of TOP I at 344 nm decreased markedly With increasing amounts of ISO to TOP I solution, while ISO did not show intrinsic fluorescence under the same experimental conditions, indicating that ISO could interact with TOP I.

The Stern–Volmer plots for the quenching of TOP I by ISO at three different temperatures are presented in Fig. 1A. Based on Equation (2), Table 1 shows that the K_{SV} values for the interaction of ISO with TOP I decreased with increasing temperature, and the corresponding K_q values were in order of 10^{12} L mol^{-1} s^{-1}, which were greater than the limiting diffusion rate constant of the biomolecule (2×10^{10} L mol^{-1} s^{-1}). It was mainly controlled by a static quenching mechanism resulting from the formation of ISO–TOP I complex [31].

Basis of Equation (3), the increasing trend of binding constant (K) with rising temperature was observed (Table 1), indicating that the capacity of ISO binding to TOP I was enhanced and the binding was an endothermic and entropy-driven reaction [32]. The number of binding sites (n) were approximately equal to 1, suggesting the existence of just a single binding site on TOP I for ISO which convincingly supported the conclusion obtained from Lineweaver–Burk Plot Analysis.

3.2. Thermodynamic analysis and the nature of the binding forces

Table 1 lists the thermodynamic parameters for the interaction of ISO with TOP I. The negative signal for ΔG° indicated the ISO–-TOP I interaction was spontaneous. The values of ΔH° and ΔS° were 17.61 ± 0.1 kJ mol^{-1} and 140.65 ± 0.22 J mol^{-1} K^{-1}, respectively, suggesting that hydrophobic interactions played predominant roles in the interaction process [33].

3.3. In-vitro enzymatic assay of ISO

TOP I assay performed by gel based assays, with a range of ISO concentrations from 0.01 to 3.0 mM. A dose dependent inhibitory profile of ISO is shown in Fig. 1B. Fig. 1B showed a better activity for ISO against the enzyme, when tested at lower concentrations of 0.01 mM, 0.05 mM, and 0.1 mM, ISO was not emerged as the good inhibitory effect on TOP I, with increasing concentration of ISO, the enzymatic activity decreased remarkably. The concentrations of ISO resulting in 50% activity lost (IC_{50}) were estimated to be 0.178 ± 0.12 mM.

3.4. Computational docking of ISO on TOP I

As shown in Fig. 2A, cluster analysis was performed using a rmsd tolerance of 2.0 Å. A total of 12 multimember conformational clusters were obtained from 20 docking runs. The most energetically favorable cluster possessed lowest energy and the most frequent locus (red histogram) was used for binding orientation analysis. Table 2 lists the binding free energy of this position, it can be seen that the calculated binding energy (−4.71 kcal mol^{-1}) was same to the predicted $\Delta G_{binding}$ (−4.83 kcal mol^{-1}), indicating that the docking result was credible. The binding energy was a little larger than ΔG° (−5.72 kcal mol^{-1}) obtained from the thermodynamic analysis at 298 K. As the molecular docking was conducted under simulation of vacuum environment, the difference of the binding energy between docking results and experiment results could be attributed to the lack of desolvation energy.

In view of the above, the docking result (Fig. 2A) showed that the binding site on TOP I for ISO was binding to the active site. Indeed, it was also observed that the binding site for ISO was close to the active site pocket (Fig. 2B), and ISO was surrounded by the residues, namely, Tyr723, Thr718, Asn352, and Arg364. Moreover, one hydroxyl group on A ring could form hydrogen bonds (green line) with residue Tyr723, indicating hydrogen bond was another

Table 1
The quenching constants (K_{SV}), binding constants (K), number of binding sites (n) and relative thermodynamic parameters for the interaction of ISO with TOP I at different temperatures.

T (K)	K_{SV} ($\times 10^4$ L mol^{-1})	R^a	K ($\times 10^4$ L mol^{-1})	n	R^b	ΔH° (kJ mol^{-1})	ΔG° (kJ mol^{-1})	ΔS° (J mol^{-1} K^{-1})
298	2.69 ± 0.02	0.9985	1.55 ± 0.02	1.00 ± 0.02	0.9998	17.61 ± 0.1	−23.93 ± 0.02	140.65 ± 0.22
304	1.98 ± 0.02	0.9988	1.78 ± 0.01	1.07 ± 0.01	0.9992		−24.77 ± 0.02	
310	1.61 ± 0.01	0.9991	2.04 ± 0.01	1.08 ± 0.01	0.9992		−25.61 ± 0.02	

[a] R is the correlation coefficient for the K_{SV} values.
[b] R is the correlation coefficient for the K values.

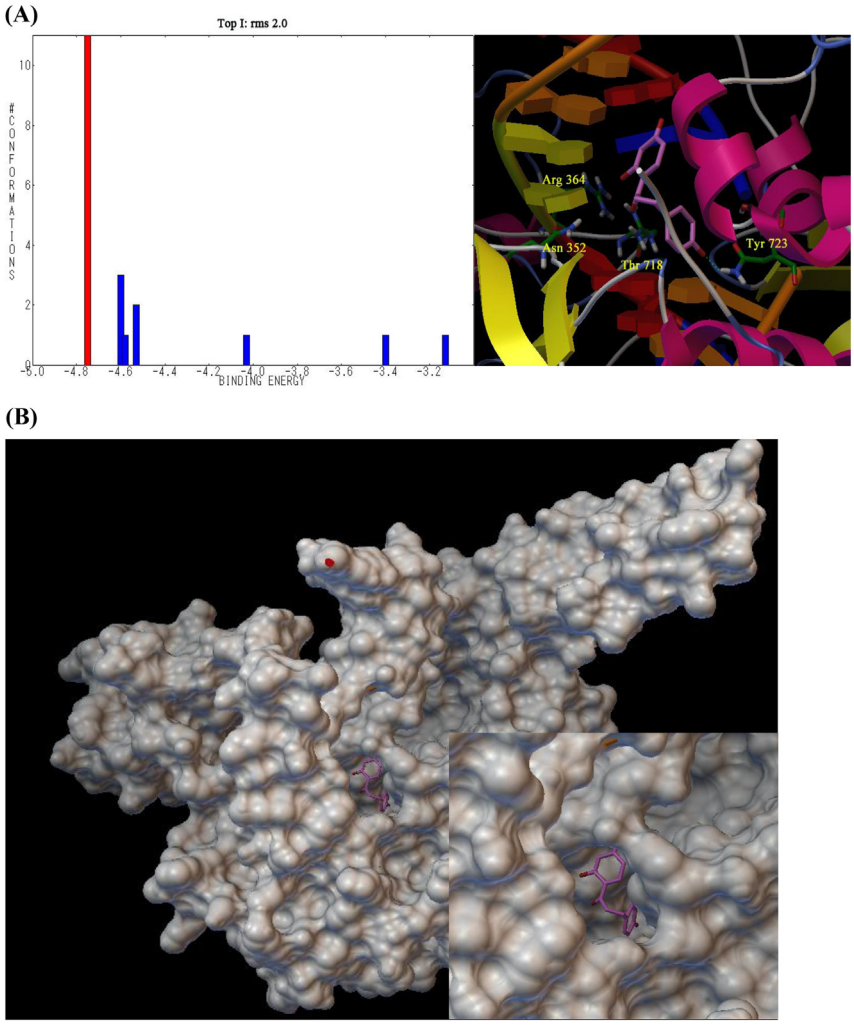

Fig. 2. (A) Cluster analysis of the AutoDock docking runs of ISO with TOP I, and the interaction between ISO and TOP I. The residues of TOP I and ISO structure were represented using stick structures; The dashed lines (green) represent hydrogen-bonding interactions. (B) Predicted binding mode of ISO docked with TOP I on molecular surface. (For interpretation of the references to colour in this figure legend, the reader is referred to the web version of this article.)

Table 2
The binding free energies of ISO and TOP I according to docking result.

Complex	Intermol energy (kcal/mol)	Internal energy (kcal/mol)	Torsional energy (kcal/mol)	Binding energy (kcal/mol)	Estimated $\Delta G_{binding}$ (kcal/mol)
ISO–TOP I	−5.20	−0.32	0.37	−4.71	−4.83

Estimated $\Delta G_{binding}$ is the sum of intermolecular energy and torsional free energy.

main role in the binding of ISO with TOP I. The docking results indicated ISO actually interacted with the amino acid residues located in the region of TOP I, which confirmed ISO as a competitive inhibitor with a single high-affinity binding site on TOP I.

3.5. In-vitro cytotoxicity screening

Fig. 3 exhibits the inhibition effect of ISO on SUN475, a concentration dependent-manner was observed in the SUN475 inhibitory activity. With increasing concentration of ISO, the SUN475 inhibitory activity decreased remarkably. The concentrations of ISO and camptothecin resulting in 50% activity lost (IC_{50}) were estimated to be 0.243 ± 0.21 and 0.238 ± 0.41 mM, respectively. The results indicated that ISO has significant SUN475 inhibitory activity compared with camptothecin.

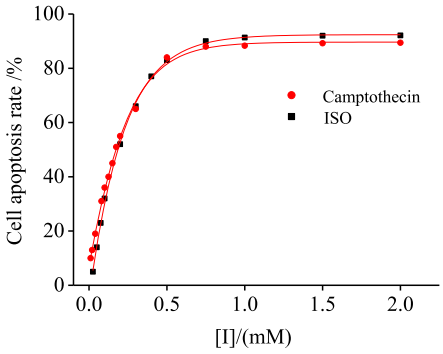

Fig. 3. Human HCC tumor cell line (SUN 475) were treated with the ISO and camptothecin for 7 days at 37 °C. The apoptosis of both treated and untreated cells was tested by MTT assay.

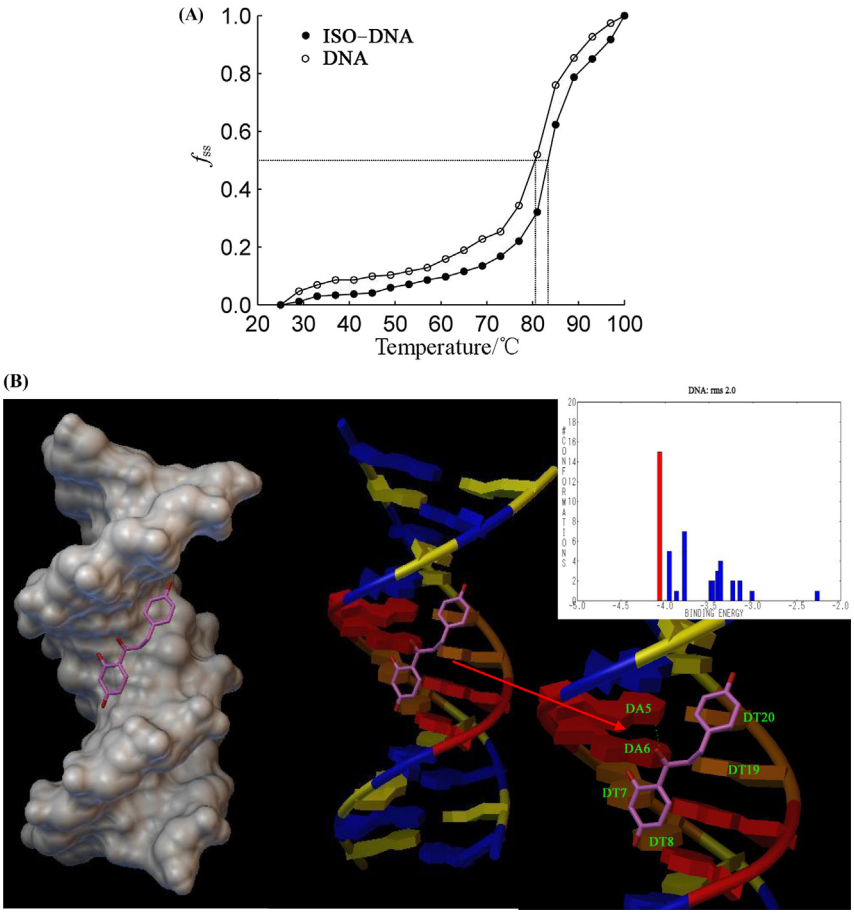

Fig. 4. (A) Melting curves of DNA in the absence and presence of ISO at pH 7.0. $c_{ISO} = 0.25$ mM, and $c_{DNA} = 0.06$ mM. (B) Cluster analyses of the AutoDock docking runs of ISO with DNA; Docking pose of the energy-minimized structure of ISO–TOP I complex.

3.6. DNA melting studies

Under the condition that DNA solutions are exposed to extremes of pH or heat, the double helical structure of DNA undergoes a transition into a randomly single-stranded form at the melting temperature (T_m). In addition, the melting temperature can be altered by the interaction of DNA with small molecules [34]. Generally, classical intercalation of small molecules into the double helix causes stabilization of base stacking and leads to a significant increase of T_m (about 5–8 °C), while non-intercalation (e.g. groove or electrostatic) binding causes no obvious increase in T_m [35]. As shown in Fig. 4A, upon the binding of ISO, the T_m value of DNA was increased from 80.6 °C to 83.2 °C and increment was smaller than 5–8 °C. Therefore, it can be deduced that ISO can interact with DNA via non-classical rather than classical intercalation.

3.7. Computational docking of ISO on DNA

Cluster analysis was performed using a rmsd tolerance of 2.0 Å. A total of 15 multimember conformational clusters were obtained from 20 docking runs. For the reason that the most energetically favorable cluster possessed lowest energy, the predicted binding model with the lowest binding energy was then used for binding orientation analysis. Fig. 4B showed the docked conformation of the ligand ISO with DNA. ISO was surrounded by DA5, DA6, DT7, DT8, DT19, and DT20. It can be observed that the aromatic ring of ISO can intercalate into the intermediate space of the two base pairs parallelly and the planar double bond vertically interact with the base pair of DNA. The docking studies gave a prediction of the interaction between ISO and DNA based on lowest energy principle. According to the results, the probable binding mode was intercalating binding and the formation of one hydrogen bonds suggested that A-T base pair may be the active binding site. It should be noted that such extracted information is unobtainable with the use of conventional methods of data interpretation. We hope that this work can benefit further understanding of the binding mechanism of ISO with DNA and comprehension ISO's pharmacological effects as well as the design of the structure of new and efficient drug molecules.

Conflict of interest

None declared.

Transparency document

Transparency document related to this article can be found online at http://dx.doi.org/10.1016/j.bbrc.2015.07.003.

References

[1] Y. Pommier, DNA topoisomerase I inhibitors: chemistry, biology, and interfacial inhibition, Chem. Rev. 109 (2009) 2894–2902.
[2] Y. Pommier, Topoisomerase I inhibitors: camptothecins and beyond, Nat. Rev. Cancer 6 (2006) 789–802.
[3] J.J. Champoux, DNA topoisomerases: structure, function, and mechanism, Ann. Rev. Biochem. 70 (2001) 369–413.

[4] L. Stewart, M.R. Redinbo, X. Qiu, W.G.J. Hol, J.J. Champoux, A model for the mechanism of human topoisomerase I, Science 279 (1998) 1534–1541.
[5] Y. Pommier, J.A. Barcelo, V.A. Rao, O. Sordet, A.G. Jobson, L. Thibaut, Z.H. Miao, J.A. Seiler, H. Zhang, C. Marchand, K. Agama, C. Redon, Repair of topoisomerase I-mediated DNA damage, Prog. Nucl. Acid Res. Mol. Biol. 81 (2006) 179–229.
[6] O. Sordet, Q.A. Khan, K.W. Kohn, Y. Pommier, Apoptosis induced by topoisomerase inhibitors, Curr. Med. Chem. Anti Cancer Agents 3 (2003) 271–290.
[7] B.L. Staker, K. Hjerrild, M.D. Feese, C.A. Behnke, A.B. Burgin, L. Stewart, The mechanism of topoisomerase I poisoning by a camptothecin analogue, Proc. Natl. Acad. Sci. U. S. A. 99 (2002) 15387–15392.
[8] J.C. Wang, Cellular roles of DNA topoisomerases: a molecular perspective, Nat. Rev. Mol. Cell. Biol. 3 (2002) 430–440.
[9] M.E. Wall, M.C. Wani, C.E. Cook, K.H. Palmer, A.T. McPhail, G.A. Sim, Plant antitumor agents. I. The isolation and structure of camptothecin, a novel Alkaloidal Leukemia and tumor inhibitor from camptotheca acuminata, J. Am. Chem. Soc. 88 (1966) 3888–3890.
[10] B. Teicher, Next generation of topoisomerase I inhibitors: rationale and biomarker strategies, Biochem. Pharmacol. 75 (2008) 1262–1271.
[11] C.J. Thomas, N.J. Rahier, S.M. Hecht, Camptothecin: current perspectives, Bioorg. Med. Chem. 12 (2004) 1585–1604.
[12] C.J. Li, L. Averboukh, A.B. Pardee, Beta-Lapachone, a novel DNA topoisomerase I inhibitor with a mode of action different from camptothecin, J. Biol. Chem. 268 (1993) 22463–22468.
[13] C. Jaxel, K.W. Kohn, M.C. Wani, Y. Pommier, Structure–activity study of the actions of camptothecin derivatives on mammalian topoisomerase I: evidence for a specific receptor site and a relation to antitumor activity, Cancer Res. 49 (1989) 1465–1469.
[14] H. Minami, J.H. Beijen, J. Verwij, M.J. Ratain, Limited sampling model for area under the concentration time curve of total Topotecan, Clin. Cancer Res. 2 (1996) 43–46.
[15] M.J. Luzzio, J.M. Besterman, D.L. Emerson, M.G. Evans, K. Lackey, P.L. Leitner, G. McIntyre, B. Morton, P.L. Myers, et al., Synthesis and antitumor-activity of novel water-soluble derivatives of camptothecin as specific inhibitors of topoisomerase-I, J. Med. Chem. 38 (1995) 395–401.
[16] Z. Mi, T.G. Burke, Differential interactions of camptothecin lactone and carboxylate forms with human blood components, Biochemistry 33 (1994) 10325–10336.
[17] Y. Urasaki, G.S. Laco, P. Pourquier, Y. Takebayashi, G. Kohlhagen, C. Gioffre, H.L. Zhang, D. Chatterjee, P. Pantazis, Y. Pommier, Characterization of a novel topoisomerase I mutation from a camptothecin-resistant human prostate cancer cell line, Cancer Res. 61 (2001) 1964–1969.
[18] A. Fujimori, W.G. Harker, G. Kohlhagen, Y. Hoki, Y. Pommier, Mutation at the catalytic site of topoisomerase I in CEM/C2, a human leukemia cell resistant to camptothecin, Cancer Res. 55 (1995) 1339–1346.
[19] S.E. Bates, W.Y. Medina-Perez, G. Kohlhagen, S. Antony, T. Nadjem, R.W. Robey, Y. Pommier, ABCG2 mediates differential resistance to SN-38 (7-Ethyl-10-hydroxycamptothecin) and homocamptothecins, J. Pharmacol. Exp. Ther. 310 (2004) 836–842.
[20] Y. Hoki, A. Fujimori, Y. Pommier, Differential cytotoxicity of clinically important camptothecin derivatives in P-glycoprotein overexpressing cell lines, Cancer Chemother. Pharmacol. 40 (1997) 433–438.
[21] M. Brangi, T. Litman, M. Ciotti, K. Nishiyama, G. Kohlhagen, C. Takimoto, R. Robey, Y. Pommier, T. Fojo, S.E. Bates, Camptothecin resistance: role of the ATP-binding cassette (ABC), mitoxantrone-resistance half-transporter (MXR), and potential for glucuronidation in MXR-expressing Cells, Cancer Res. 59 (1999) 5938–5946.
[22] D.K. Armstrong, Topotecan dosing guidelines in ovarian cancer: reduction and management of hematologic toxicity, Oncologist 9 (2004) 33–42.
[23] L.B. Saltz, Clinical use of irinotecan: current status and future considerations, Oncologist 2 (1997) 402–409.
[24] S.Y. Bi, Y.T. Sun, C.Y. Qiao, H.Q. Zhang, C.M. Liu, Binding of several anti-tumor drugs to bovine serum albumin: fluorescence study, J. Lumin 129 (2009) 541–547.
[25] Y.Q. Li, F.C. Zhou, F. Gao, J.S. Bian, F. Shan, Comparative evaluation of quercetin, isoquercetin and rutin as inhibitors of α-glucosidase, J. Agric. Food Chem. 57 (2009) 11463–11468.
[26] G.W. Zhang, L. Wang, J.H. Pan, Probing the binding of the flavonoid diosmetin to human serum albumin by multispectroscopic techniques, J. Agric. Food Chem. 60 (2012) 2721–2729.
[27] M. Liu, W. Zhang, L. Qiu, X.K. Lin, Synthesis of butyl-isobutyl-phthalate and its interaction with α-glucosidase in vitro, J. Biochem. 149 (2011) 27–33.
[28] A.A. Godbole, M.N. Leelaram, A.G. Bhat, P. Jain, V. Nagaraja, Characterization of DNA topoisomerase I from mycobacterium tuberculosis: DNA cleavage and relegation properties and inhibition of its activity, Arch. Biochem. Biophys. 528 (2012) 197–203.
[29] H.M. Berman, J. Westbrook, Z.K. Feng, G. Gilliland, T.N. Bhat, H. Weissig, L.N. Shindyalov, P.E. Bourne, The protein data bank, Nucl. Acid Res. 28 (2000) 235–242.
[30] C.G. Ricci, P.A. Netz, Docking studies on DNA-ligand interactions: building and application of a protocol to identify the binding mode, J. Chem. Inf. Model 49 (2009) 1925–1935.
[31] H. Zhang, R.T. Liu, Z.X. Chi, C.Z. Gao, Toxic effects of different charged metal ions on the target-Bovine serum albumin, Spectrochim. Acta Part A 78 (2011) 523–527.
[32] G.W. Zhang, Y.D. Ma, L. Wang, Y.P. Zhang, J. Zhou, Multispectroscopic studies on the interaction of maltol, a food additive, with bovine serum albumin, Food Chem. 133 (2012) 264–270.
[33] P.D. Ross, S. Subramanian, Thermodynamics of protein association reactions: forces contributing to stability, Biochemistry 20 (1981) 3096–3102.
[34] Y.D. Ma, G.W. Zhang, J.H. Pan, Spectroscopic studies of DNA interaction with food colorant indigo carmine with the use of ethidium bromide as a fluorescence probe, J. Agric. Food Chem. 60 (2012) 10867–10875.
[35] Y.T. Sun, H.Q. Zhang, S.Y. Bi, X.F. Zhou, L. Wang, Y.S. Yan, Studies on the arctilin and its interaction with DNA by spectral methods, J. Lumin. 131 (2011) 2299–2306.